PNAS
www.pnas.org

Supplementary Information for

An ErbB2 splice variant lacking exon 16 drives lung carcinoma

Harvey W. Smith, Lei Yang, Chen Ling, Arlan Walsh, Victor D. Martinez, Jonathan Boucher, Dongmei Zuo, Ethan S Sokol, Dean C Pavlick, Garrett M Frampton, Juliann Chmielecki, Laura M. Jones, Philippe Roux, William W. Lockwood and William J. Muller

Corresponding Authors: Prof. William J. Muller, Dr. Harvey W. Smith

Email: william.muller@mcgill.ca, harvey.smith2@mcgill.ca

This PDF file includes:

Figs. S1 to S5

www.pnas.org/cgi/doi/10.1073/pnas.2007474117

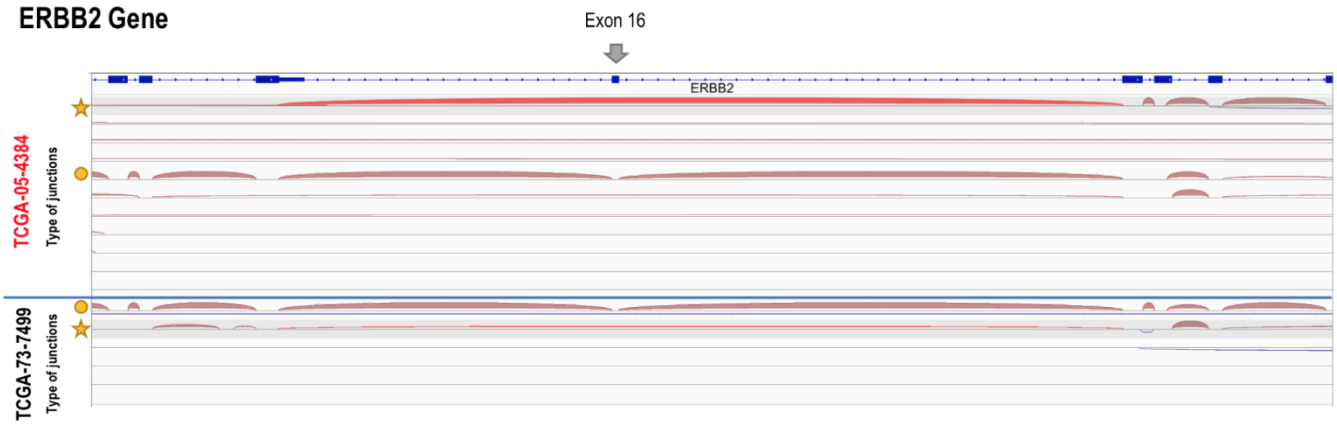

SI Figure 1: Detailed splice junction scheme for TCGA-05-4384 and TCGA-73-7499. Visualization of representative RNA-Seq data from patients in TCGA with ERBB2 splicing mutations (TCGA-05-4384 – upper panel) and wild-type ERBB2 (TCGA-73-749 – lower panel). Sub-tracks represent the different types and abundance of splice junctions observed in each sample. The two sub-tracks containing junctions skipping exon 16 are highlighted in red. Splice junctions skipping exon 16 (indicated with a star) represent the dominant type of junction in the sample containing the mutation, while only representing a minor fraction in the non-mutated sample. The expected pattern of splice junctions is indicated by a circle.

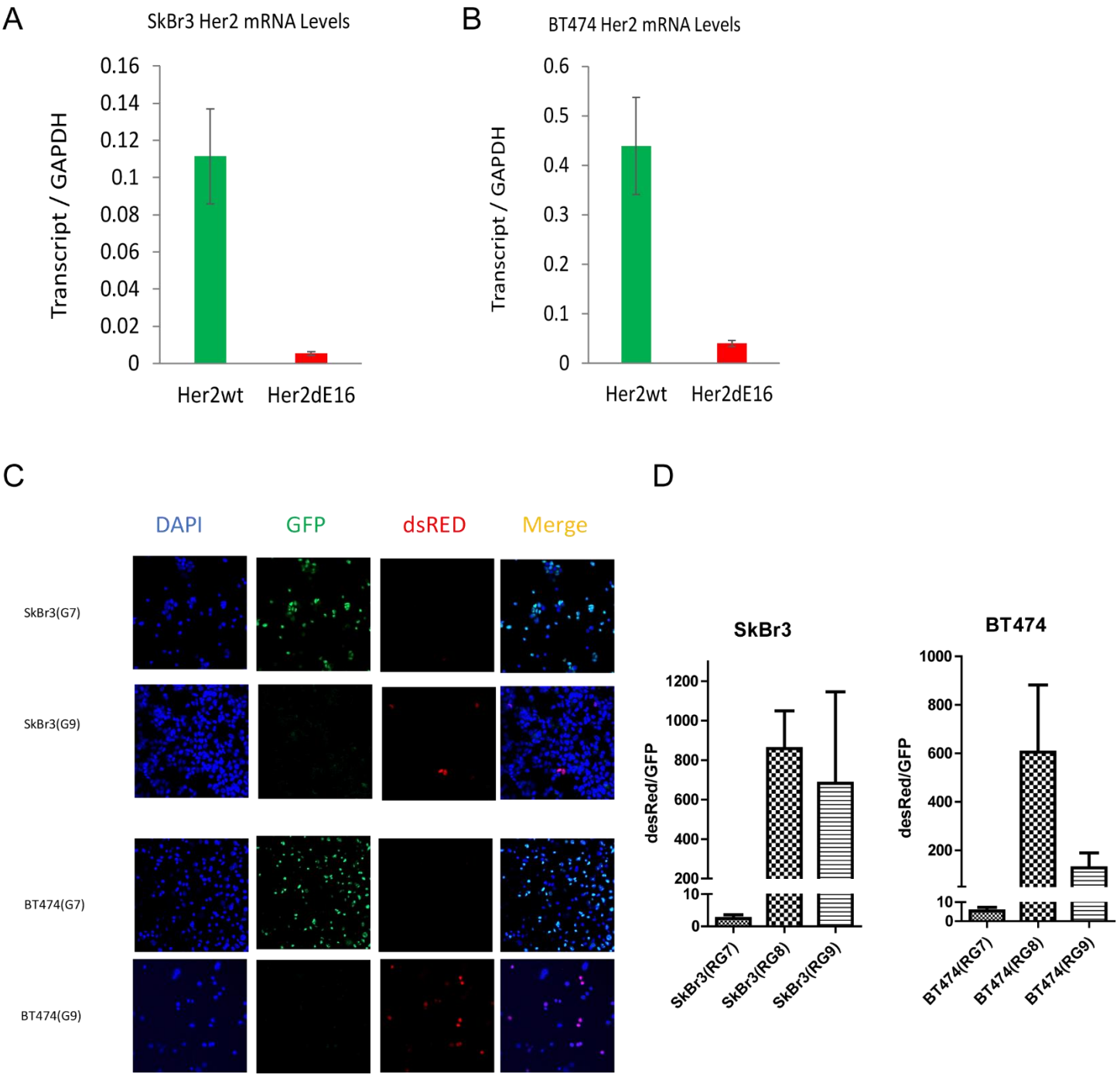

SI Figure 2: Splice acceptor site mutations at the *ERBB2* intron15/exon16 junction cause constitutive exon 16 skipping. (A) Endogenous expression of full-length ERBB2 (Her2wt) and ERBB2ΔEx16 (Her2dE16) splice isoforms of ERBB2 in SkBr3 breast carcinoma cells (A) or BT474 breast carcinoma cells (B) was determined using qRT-PCR with normalization to the housekeeping gene *GAPDH*. **(C)** SkBr3 (top panels) or BT474 (bottom panels) cells were transfected with the splicing reporter construct RG9 and control RG7. GFP and dsRed fluorescence were observed using confocal microscopy **(D)** Corresponding transcripts were quantified using qRT-PCR and compared to data generated using splicing reporter construct RG8 (Figure 3).

A

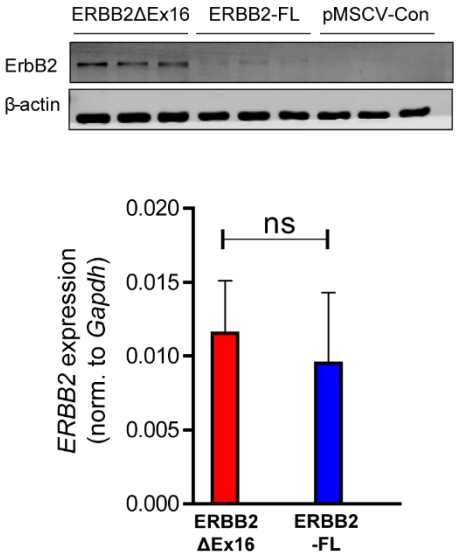

B

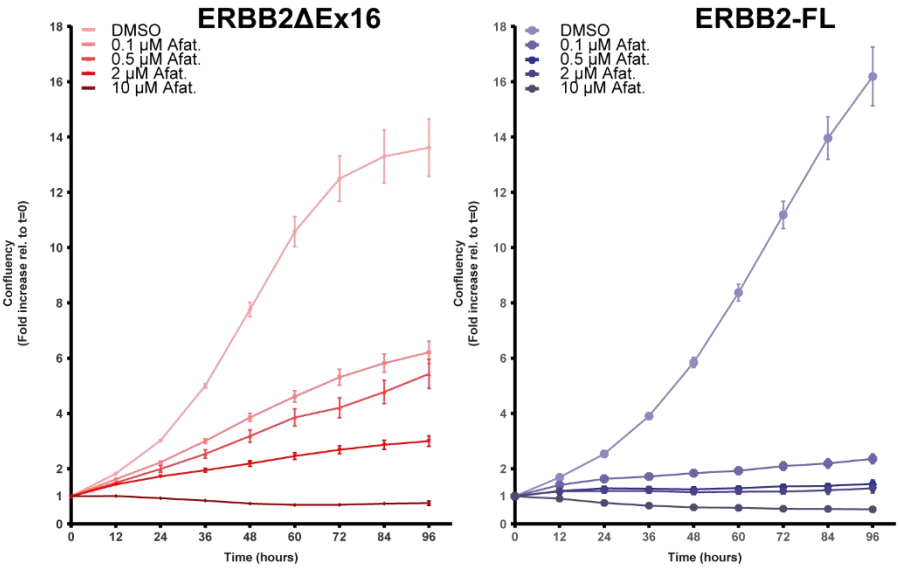

C

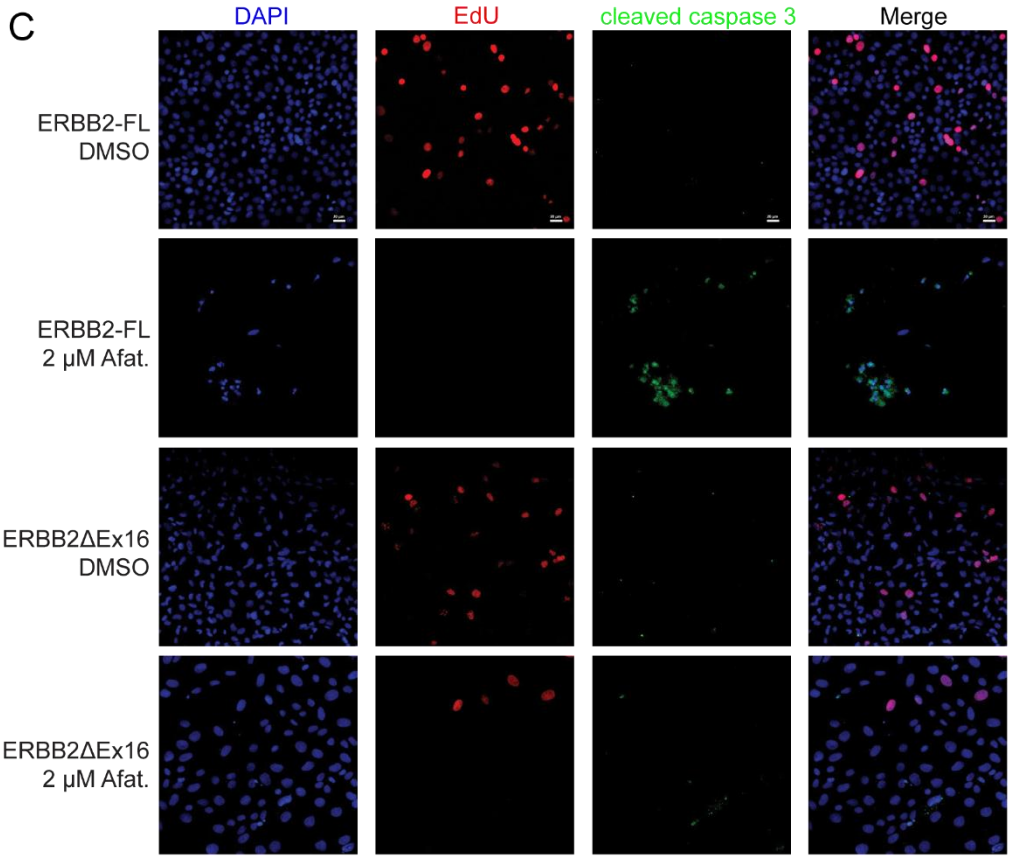

D

	Subcutaneous	Mammary Fat Pad
pMSCV Control	0/4	0/8
ERBB2-FL	0/4	0/8
ERBB2ΔEx16	4/4	8/8

E

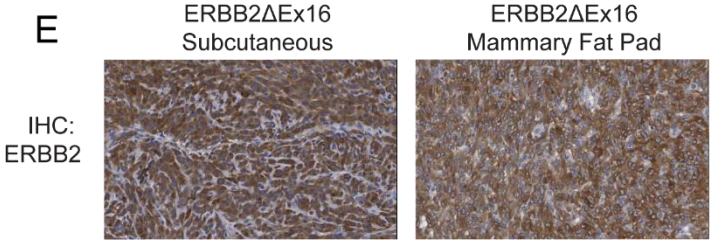

SI Figure 3: ERBB2 expression, TKI responses and tumorigenic capacity of RLE-6TN stable cell lines expressing ERBB2-FL or ERBB2ΔEx16. (A) Upper panels – immunoblots showing ERBB2 protein expression in RLE-6TN cells stably expressing ERBB2-FL or ERBB2ΔEx16 or cells transduced with a vector control (pMSCV-Con). β-actin was used as a loading control. Three independently transduced cell populations per retroviral vector were analyzed. Lower panel – QRT-PCR analysis of *ERBB2* mRNA expression, normalized to *Gapdh*, in RLE-6TN cells transduced with retroviruses bearing ERBB2-FL or ERBB2ΔEx16. Data are from two independent experiments performed in quadruplicate, mean +/- SEM. ns = not significant (unpaired, two-tailed Student's t-test). **(B)** Proliferation of RLE-6TN cells stably expressing ERBB2-FL or ERBB2ΔEx16 and treated with DMSO or Afatininb as indicated was monitored by real-time image-based assessment of cell confluency over 96h. Data were normalized to cell confluency at the beginning of the assay (t=0) and are mean +/- SEM of two independent experiments, each with six replicates per condition. **(C)** RLE-6TN stable cell lines were treated with 2μM Afatinib or DMSO for 24h and immunofluorescently stained to detect cleavage of Caspase-3 and EdU incorporation. Images are representative of the data shown in Fig. 4C-D. Scale bar represents 20 μm. **(D-E)** RLE-6TN cells stably expressing ERBB2-FL or ERBB2ΔEx16 or cells transduced with a vector control (pMSCV-Control) were injected subcutaneously or into the left inguinal mammary fat pads of immunocompromised (NCr) mice. Mice were monitored for tumour initiation by physical palpation. The table in (D) indicates the number of mice in each experimental group that developed tumours. Representative immunohistochemical staining to detect ERBB2 expression in tumours arising from ERBB2ΔEx16-expressing cells at at both sites is shown in (E).

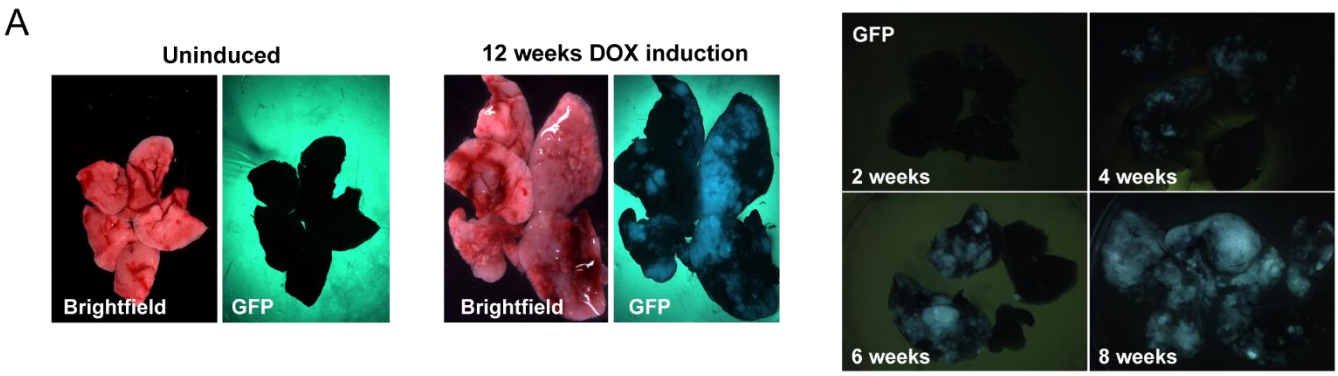
A
Uninduced
12 weeks DOX induction
Brightfield
GFP
Brightfield
GFP
GFP
2 weeks
4 weeks
6 weeks
8 weeks

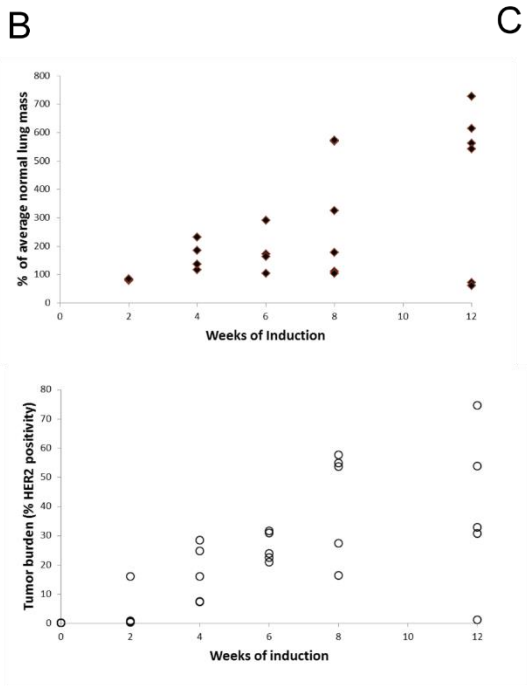
B
% of average normal lung mass
Weeks of Induction
Tumor burden (% HER2 positivity)
Weeks of induction

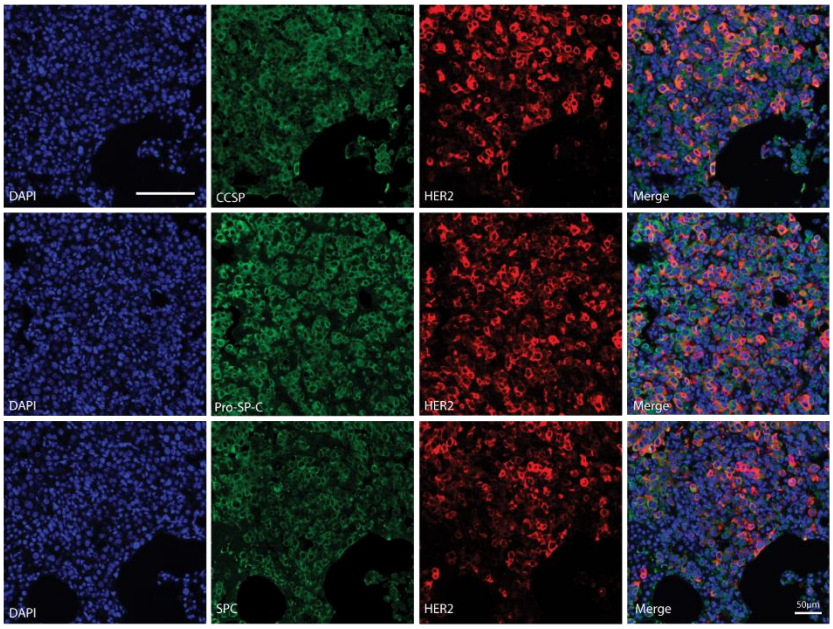
C
DAPI
CCSP
HER2
Merge
DAPI
Pro-SP-C
HER2
Merge
DAPI
SPC
HER2
Merge
50μm

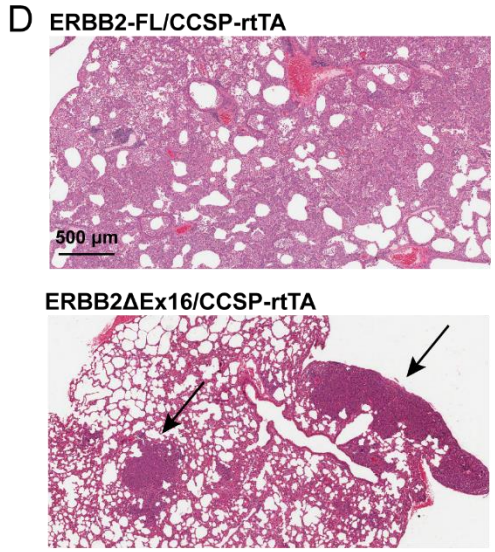
D
ERBB2-FL/CCSP-rtTA
500 μm
ERBB2ΔEx16/CCSP-rtTA

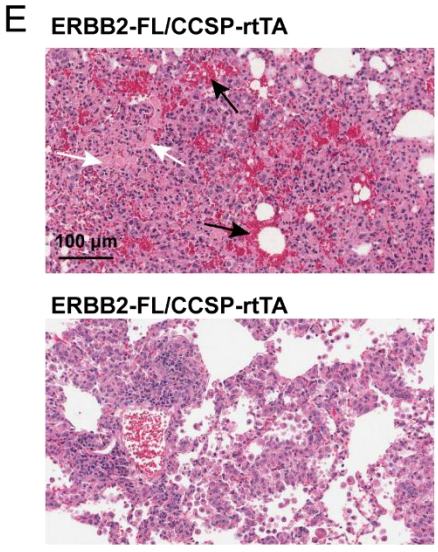
E
ERBB2-FL/CCSP-rtTA
100 μm
ERBB2-FL/CCSP-rtTA

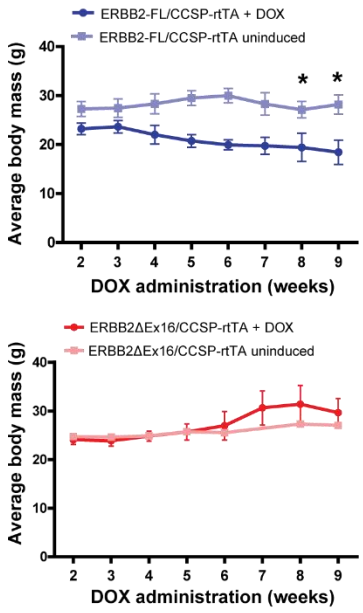
F
ERBB2-FL/CCSP-rtTA + DOX
ERBB2-FL/CCSP-rtTA uninduced
Average body mass (g)
DOX administration (weeks)
ERBB2ΔEx16/CCSP-rtTA + DOX
ERBB2ΔEx16/CCSP-rtTA uninduced
Average body mass (g)
DOX administration (weeks)

SI Figure 4: **Phenotypes of GEMMs expressing doxycycline-inducible ERBB2-FL or ERBB2ΔEx16 in the lung epithelium. (A)** Left panels – lungs from ErbB2ΔEx16-IRES-GFP/CCSP-rtTA mice that had been induced for 12 weeks with doxycycline and age-matched uninduced controls were whole-mounted and imaged using brightfield and fluorescence microscopy for GFP detection. Right panels – lungs from ErbB2ΔEx16-IRES-GFP/CCSP-rtTA mice that had received doxycycline for the indicated times were excised and imaged using fluorescence microscopy to detect GFP. **(B)** Doxycycline was administered to ErbB2ΔEx16-IRES-GFP/CCSP-rtTA mice, which were sacrificed at the indicated time points post-induction. Upper panel - lungs were excised and weighed at their mass was compared to an average lung mass of age-matched control mice (without doxycycline administration). Lower panel - ERBB2 (HER2) immunohistochemistry was performed on FFPE sections of lung tissue and the percentage of epithelial cells staining positively for ERBB2 expression was calculated using image analysis software (Aperio ImageScope). **(C)** Immunofluorescence showing ERBB2 (HER2), CCSP, Pro-SP-C and SP-C expression in the lungs of ERBB2ΔEx16/CCSP-rtTA mice after 3 weeks of doxycycline administration. DAPI was used as a nuclear counterstain. Images representative of observations from five mice. Scale bar represents 100 μm. **(D)** Representative low-magnification H&E images of lung tissue sections from mice receiving doxycycline for 12 weeks. Top panel shows widespread loss of normal alveolar architecture in ERBB2-FL/CCSP-rtTA mice. Bottom panel shows focal tumour masses in the lungs of ERBB2ΔEx16/CCSP-rtTA mice (black arrows). Scale bar represents 500 μm. **(E)** H&E images of lungs from ERBB2-FL/CCSP-rtTA mice taken at higher magnification reveal features associated with inflammation, including hemorrhage (black arrows) and accumulation of proteinaceous fluid (white arrows), with destruction of normal lung architecture and abundant leukocyte infiltration visible throughout the sections. Scale bar represents 100 μm. **(F)** Average body mass of ERBB2-FL/CCSP-rtTA and ERBB2ΔEx16/CCSP-rtTA mice with and without doxycycline administration (n=8/group). Mean +/- SEM, * = $p<0.05$, unpaired, two-tailed Student's t-test.

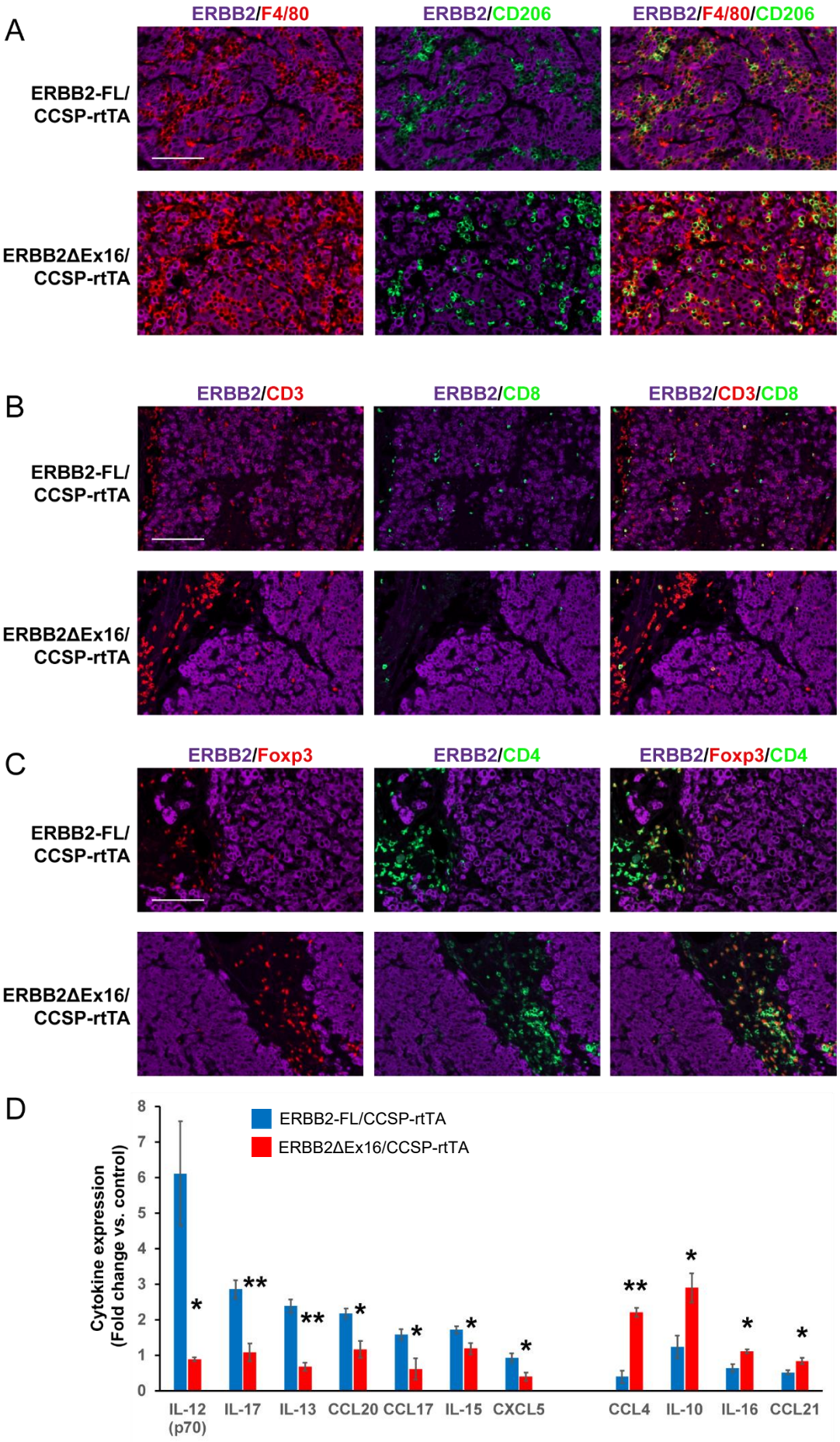
A
ERBB2/F4/80
ERBB2/CD206
ERBB2/F4/80/CD206
ERBB2-FL/
CCSP-rtTA
ERBB2ΔEx16/
CCSP-rtTA
B
ERBB2/CD3
ERBB2/CD8
ERBB2/CD3/CD8
ERBB2-FL/
CCSP-rtTA
ERBB2ΔEx16/
CCSP-rtTA
C
ERBB2/Foxp3
ERBB2/CD4
ERBB2/Foxp3/CD4
ERBB2-FL/
CCSP-rtTA
ERBB2ΔEx16/
CCSP-rtTA
D
ERBB2-FL/CCSP-rtTA
ERBB2ΔEx16/CCSP-rtTA
Cytokine expression
(Fold change vs. control)
0
1
2
3
4
5
6
7
8
IL-12
(p70)
IL-17
IL-13
CCL20
CCL17
IL-15
CXCL5
CCL4
IL-10
IL-16
CCL21

SI Figure 5: **ErbB2ΔEx16-driven lung tumors exhibit evidence of a pro-tumor, immunosuppressive microenvironment**. **(A-C)** ERBB2ΔEx16/CCSP-rtTA mice were treated with doxycycline for 12 weeks and lung tumor sections were immunofluorescently stained with the indicated antibodies to confirm ERBB2 (HER2) expression and to identify immune cells in the tumor microenvironment. DAPI was used as a nuclear counterstain. Images are representative of lungs from 5 mice/genotype. Scale bar indicates 100μm. **(D)** Serum cytokine levels in ERBB2-FL/CCSP-rtTA (blue bars) and ERBB2ΔEx16/CCSP-rtTA (red bars) mice after 4 weeks of doxycycline induction. Data are mean +/- SEM (n=4 mice per genotype) of fold change relative to mean values from uninduced mice (n=2) of each genotype. * = $p<0.05$, ** = $p<0.01$, unpaired, two-tailed Student's t-test. While 44 cytokines were analyzed in total, only those with significantly different levels in serum from the two strains are shown.